

Analysis of discrete energy-decay preserving schemes for Maxwell's equations in Cole-Cole dispersive medium

Guoyu Zhang^{a,b}, Ziming Dong^c, Baoli Yin^{a,b,*}, Yang Liu^{a,b}, Hong Li^{a,b}

^a*School of Mathematical Sciences, Inner Mongolia University, Hohhot 010021, China;*

^b*Inner Mongolia Key Laboratory of Mathematical Modeling and Scientific Computing, Hohhot 010021, China;*

^c*Faculty of Mathematics, Baotou Teachers' College, Baotou 014030, China;*

Abstract

This work investigates the design and analysis of energy-decay preserving numerical schemes for Maxwell's equations in a Cole-Cole (C-C) dispersive medium. A continuous energy-decay law is first established for the C-C model through a modified energy functional. Subsequently, a novel θ -scheme is proposed for temporal discretization, which is rigorously proven to preserve a discrete energy dissipation property under the condition $\theta \in [\frac{\alpha}{2}, \frac{1}{2}]$. The temporal convergence rate of the scheme is shown to be first-order for $\theta \neq 0.5$ and second-order for $\theta = 0.5$. Extensive numerical experiments validate the theoretical findings, including convergence tests and energy-decay comparisons. The proposed SFTR- θ scheme demonstrates superior performance in maintaining monotonic energy decay compared to an alternative 2nd-order fractional backward difference formula, particularly in long-time simulations, highlighting its robustness and physical fidelity.

Keywords: Maxwell's equations, Cole-Cole dispersive medium, energy-decay, SFTR- θ , θ method

2010 MSC: 65N06, 65B99.

1. Introduction

The study of wave propagation in dispersive media such as water, soil, biological tissue, the ionosphere, plasma, optical fibers, and radar-absorbing materials has been an active area of engineering research since the early 1990s, motivated by the common characteristic of frequency-dependent permittivity or permeability in these materials [1, 2, 3, 4, 5, 6]. To characterize this frequency-domain behavior, various constitutive models have been developed, including the Drude model [7], the Lorenz model [8], and several anomalously dispersive models such as the Havriliak-Negami model [9, 10] and the Cole-Cole (C-C) model [11]. Numerical simulation of wave propagation in such media has been addressed through multiple time-domain discretization techniques. These include finite-difference time-domain (FDTD) [12, 13, 14, 15, 16, 17], finite element time-domain (FETD) [2, 18, 19, 20], spectral time-domain (STD) [21, 22], and discontinuous Galerkin time-domain (DGTD) [23, 24] methods. Complementary frequency-domain formulations have also been explored, as documented in [25, 26, 27, 28, 29] and related references.

*Corresponding author

Email addresses: guoyu_zhang@imu.edu.cn (Guoyu Zhang), dong88math@163.com (Ziming Dong), baolimath@126.com (Baoli Yin), mathliuyang@imu.edu.cn (Yang Liu), smslh@imu.edu.cn (Hong Li)

The 2-D Maxwell's equations in a Cole-Cole dispersive medium [2] can be stated as

$$\epsilon_0 \epsilon_\infty \frac{\partial \mathbf{E}}{\partial t}(\mathbf{x}, t) = \nabla \times H(\mathbf{x}, t) - \frac{\partial \mathbf{P}}{\partial t}(\mathbf{x}, t), \quad (1)$$

$$\mu_0 \frac{\partial H}{\partial t}(\mathbf{x}, t) = -\nabla \times \mathbf{E}(\mathbf{x}, t), \quad (2)$$

$$\tau_0^\alpha \partial_t^\alpha \mathbf{P}(\mathbf{x}, t) + \mathbf{P}(\mathbf{x}, t) = \epsilon_0(\epsilon_s - \epsilon_\infty) \mathbf{E}(\mathbf{x}, t), \quad (3)$$

where $(\mathbf{x}, t) \in \Omega \times (0, T)$ for some $T > 0$ and $\mathbf{x} = (x, y) \in \Omega = (a, b) \times (c, d)$. The electric field $\mathbf{E}(\mathbf{x}, t) = (E_1, E_2)^\top$ and the magnetic field $H(\mathbf{x}, t)$ are the primary electromagnetic quantities in the model, while $\mathbf{P}(\mathbf{x}, t)$ denotes the time-domain polarization field. The material parameters include the free-space permittivity ϵ_0 , the infinite-frequency permittivity ϵ_∞ , and the static permittivity ϵ_s , which satisfy the physical constraint $\epsilon_s > \epsilon_\infty$. Additionally, μ_0 represents the free-space permeability, and τ_0 is the relaxation time. The curl operators are defined as follows:

$$\nabla \times H = \left(\frac{\partial H}{\partial y}, -\frac{\partial H}{\partial x} \right)^\top, \quad \nabla \times \mathbf{E} = \frac{\partial E_2}{\partial x} - \frac{\partial E_1}{\partial y}.$$

To complete the initial-boundary value problem described by equations (1)–(3), the following initial and boundary conditions are imposed:

$$\mathbf{E}(\mathbf{x}, 0) = \mathbf{E}_0(\mathbf{x}), \quad H(\mathbf{x}, 0) = H_0(\mathbf{x}), \quad \mathbf{P}(\mathbf{x}, 0) = \mathbf{0}, \quad \mathbf{x} \in \overline{\Omega}, \quad (4)$$

and

$$\mathbf{n} \times \mathbf{E} = \mathbf{0} \quad \text{on } \partial\Omega \times [0, T], \quad (5)$$

where \mathbf{n} is the outward unit normal vector to the boundary $\partial\Omega$. The operator ∂_t^α represents the α th fractional differential operator in Caputo sense, i.e., $\partial_t^\alpha u = \mathcal{I}^{1-\alpha} u_t$ where \mathcal{I}^α denotes the Riemann-Liouville fractional integral operator of order α , defined by

$$(\mathcal{I}^\alpha u)(t) = \frac{1}{\Gamma(\alpha)} \int_0^t \frac{u(s) ds}{(t-s)^{1-\alpha}}. \quad (6)$$

In their work [2], Li et al. established that the C-C model described by equations (1)–(5) satisfies the following energy stability property:

$$\mathcal{E}(t) \leq \mathcal{E}(0), \quad \text{for all } t \in [0, T],$$

where the energy functional is defined as

$$\mathcal{E}(t) = \epsilon_0(\epsilon_s - \epsilon_\infty) (\epsilon_0 \epsilon_\infty \|\mathbf{E}(t)\|^2 + \mu_0 \|H(t)\|^2) + \|\mathbf{P}(t)\|^2.$$

Subsequently, the authors of [30] provided, for the first time, a sufficient condition for determining when a second-order accurate discrete scheme can preserve such an energy stability property. See also the related work [31]. Nevertheless, it remains an important objective to define an appropriate energy functional that exhibits monotonic decay over time, and to develop numerical schemes that preserve this energy-decay behavior. Such an energy functional is particularly valuable in the design of adaptive time-stepping strategies, as the rate of energy-decay can serve as an effective criterion for dynamically adjusting the time step size. In light of this, the contributions of this paper can be summarized as follows:

- A rigorous proof of the energy-decay law for the Cole-Cole model is established.
- A θ -scheme is designed and theoretically demonstrated to preserve the discrete energy-decay property.
- Comprehensive numerical experiments are provided to validate the theoretical findings.

This paper is organized as follows. Section 2 establishes the energy-decay law for the Cole-Cole model through the introduction of a modified energy functional. In Section 3, we propose a θ -scheme and demonstrate its capability to preserve the discrete energy-decay property by proving several essential characteristics of the method. A comprehensive error analysis for the temporally semi-discrete scheme is presented in Section 4, while extensive numerical validation is provided in Section 5. The paper concludes with final remarks in Section 6.

This section concludes with essential notation and assumptions. Let C denote a generic positive constant, independent of the mesh sizes h and τ , whose value may vary in different contexts. For $r \geq 0$, $H^r(\Omega)$ denotes the standard Sobolev space with norm $\|\cdot\|_r$ and seminorm $|\cdot|_r$. Here, $\|\cdot\|$ abbreviates $\|\cdot\|_0$, and $H^0(\Omega)$ coincides with $L^2(\Omega)$. Define the space

$$H^r(\text{curl}; \Omega) = \{ \mathbf{v} \in (H^r(\Omega))^2 : \nabla \times \mathbf{v} \in H^r(\Omega) \}, \quad \|\mathbf{v}\|_{r,\text{curl}} = (\|\mathbf{v}\|_r^2 + \|\nabla \times \mathbf{v}\|_r^2)^{1/2},$$

and its subspace

$$H_0(\text{curl}; \Omega) = \{ \mathbf{v} \in H(\text{curl}; \Omega) : \mathbf{n} \times \mathbf{v} = 0 \text{ on } \partial\Omega \},$$

where $H(\text{curl}; \Omega) = H^0(\text{curl}; \Omega)$. We assume the solution \mathbf{P} satisfies the regularity condition: for almost every $\mathbf{x} \in \Omega$, $\partial_t \mathbf{P}(\mathbf{x}, t) \in L^1(0, T)$ and $\partial_t^\alpha \mathbf{P}(\mathbf{x}, t) \in C[0, T]$. Under this assumption, the following identities (see [32, Theorem 2.14]) and inequality (see [33, 34]) hold:

$$\partial_t \mathbf{P} = {}_{RL}\partial_t^{1-\alpha} (\mathcal{I}^{1-\alpha} \partial_t \mathbf{P}) = {}_{RL}\partial_t^{1-\alpha} (\partial_t^\alpha \mathbf{P}), \quad (7)$$

and

$$\partial_t^\alpha \mathbf{P}(t) \cdot [{}_{RL}\partial_t^{1-\alpha} (\partial_t^\alpha \mathbf{P})] (t) \geq \frac{1}{2} [{}_{RL}\partial_t^{1-\alpha} (\partial_t^\alpha \mathbf{P})^2] (t) + \frac{1}{2} \eta_\alpha(t) (\partial_t^\alpha \mathbf{P}(t))^2, \quad (8)$$

where $\eta_\alpha(t) = \frac{t^{\alpha-1}}{\Gamma(\alpha)}$, and ${}_{RL}\partial_t^\alpha u = \frac{d}{dt} \mathcal{I}^{1-\alpha} u$ denotes the Riemann–Liouville fractional derivative of order α .

2. Continuous energy dissipation

The weak formulation of (1)-(3) can be formulated as: Find $\mathbf{E} \in C(0, T; H_0(\text{curl}; \Omega)) \cap C^1(0, T; (L^2(\Omega))^2)$, $H \in C^1(0, T; L^2(\Omega))$ and $\mathbf{P} \in C^1(0, T; (L^2(\Omega))^2)$ so that

$$\epsilon_0 \epsilon_\infty \left(\frac{\partial \mathbf{E}}{\partial t}, \boldsymbol{\chi} \right) + \left(\frac{\partial \mathbf{P}}{\partial t}, \boldsymbol{\chi} \right) - (H, \nabla \times \boldsymbol{\chi}) = 0, \quad \forall \boldsymbol{\chi} \in H_0(\text{curl}; \Omega), \quad (9)$$

$$\mu_0 \left(\frac{\partial H}{\partial t}, \phi \right) + (\nabla \times \mathbf{E}, \phi) = 0, \quad \forall \phi \in L^2(\Omega), \quad (10)$$

$$\tau_0^\alpha (\partial_t^\alpha \mathbf{P}, \boldsymbol{\psi}) + (\mathbf{P}, \boldsymbol{\psi}) - \epsilon_0 (\epsilon_s - \epsilon_\infty) (\mathbf{E}, \boldsymbol{\psi}) = 0, \quad \forall \boldsymbol{\psi} \in (L^2(\Omega))^2. \quad (11)$$

For a better explanation of the definition of compatible energy, we shall present first the energy dissipation law of the classical Debye model (i.e., by setting $\alpha = 1$ in (3) or (11)).

Lemma 2.1. (Energy dissipation of Debye model of order 1) Let $\alpha = 1$ in (11). There holds

$$\frac{d}{dt}\mathcal{E}(t) + \tau_0\|\partial_t\mathbf{P}\|^2 \leq 0, \quad (12)$$

where $\mathcal{E}(t) := \tau_0 \int_0^t \|\partial_t\mathbf{P}(s)\|^2 ds + \|\mathbf{P}\|^2 + \epsilon_0(\epsilon_s - \epsilon_\infty)(\epsilon_0\epsilon_\infty\|\mathbf{E}\|^2 + \mu_0\|H\|^2)$ and therefore,

$$\mathcal{E}(t_1) \leq \mathcal{E}(t_2), \quad \text{for } t_1 \geq t_2. \quad (13)$$

Proof. Let $\chi = \mathbf{E}$ in (9) and $\phi = H$ in (10), and add these two resultants together to obtain

$$\frac{1}{2}\epsilon_0\epsilon_\infty\frac{d}{dt}\|\mathbf{E}\|^2 + \frac{1}{2}\mu_0\frac{d}{dt}\|H\|^2 + \left(\frac{\partial\mathbf{P}}{\partial t}, \mathbf{E}\right) = 0. \quad (14)$$

Multiplying both sides of (14) by $\epsilon_0(\epsilon_s - \epsilon_\infty)$, and adding the resultant to the equation (11) after replacing ψ with $\frac{\partial\mathbf{P}}{\partial t}$, one can readily arrive at (12). Then, (13) follows for $\frac{d}{dt}\mathcal{E}(t) \leq 0$ by (12), which completes the proof of the lemma. \square

Lemma 2.2. (Energy dissipation of Cole-Cole model) For arbitrary $\alpha \in (0, 1)$, there holds

$$\frac{d}{dt}\mathcal{E}_\alpha(t) + \tau_0^\alpha\eta_\alpha(t)\|\partial_t^\alpha\mathbf{P}\|^2 \leq 0, \quad (15)$$

where $\mathcal{E}_\alpha(t) := \tau_0^\alpha\mathcal{I}^\alpha\|\partial_t^\alpha\mathbf{P}\|^2 + \|\mathbf{P}\|^2 + \epsilon_0(\epsilon_s - \epsilon_\infty)(\epsilon_0\epsilon_\infty\|\mathbf{E}\|^2 + \mu_0\|H\|^2)$ and therefore,

$$\mathcal{E}_\alpha(t_1) \leq \mathcal{E}_\alpha(t_2), \quad \text{for } t_1 \geq t_2. \quad (16)$$

Proof. Replacing ψ by $\frac{\partial\mathbf{P}}{\partial t}$ in (11), multiplying both sides of (14) by $\epsilon_0(\epsilon_s - \epsilon_\infty)$, and adding these two resultants together, one gets

$$\tau_0^\alpha(\partial_t^\alpha\mathbf{P}, \partial_t\mathbf{P}) + \frac{1}{2}\frac{d}{dt}\|\mathbf{P}\|^2 + \frac{1}{2}\epsilon_0^2\epsilon_\infty(\epsilon_s - \epsilon_\infty)\frac{d}{dt}\|\mathbf{E}\|^2 + \frac{1}{2}\mu_0\epsilon_0(\epsilon_s - \epsilon_\infty)\frac{d}{dt}\|H\|^2 = 0. \quad (17)$$

Then, (15) follows in accordance to (7), (8) and (17), and (16) is due to the monotonicity of the function $\mathcal{E}_\alpha(t)$ by (15). \square

Remark 2.3. Clearly, the term $\mathcal{I}^\alpha u$ tends to $\int_0^t u(s)ds$ and $\eta_\alpha(t) = \frac{t^{\alpha-1}}{\Gamma(\alpha)} \rightarrow 1$ when $\alpha \rightarrow 1$, and therefore, (15) extends (12) to the fractional case naturally. The energy $\mathcal{E}_\alpha(t)$ is thus regarded as being compatible with the original one $\mathcal{E}(t)$.

3. Discrete energy dissipation

In temporal direction we approximate the Maxwell's equations based on a uniform mesh with grid points: $0 = t_0 < t_1 < \dots < t_N = T$ with $t_n = n\tau$ and $\tau = \frac{T}{N}$. Let $u^n := u(t_n)$ for brevity. Introduce the following symbols

$$\partial_\tau^{n-\theta}u := \frac{u^n - u^{n-1}}{\tau}, \quad \bar{u}^{n-\theta} := (1 - \theta)u^n + \theta u^{n-1}. \quad (18)$$

as approximation to u_t and u at time $t_{n-\theta}$, respectively. To approximate the term $\partial_t^\alpha u(t_{n-\theta})$, we adopt the shifted fractional trapezoidal rule [35, 36], i.e., let

$$\partial_\tau^\alpha u^{n-\theta} := \tau^{-\alpha} \sum_{k=1}^n \omega^{n-k} (u^k - u^0), \quad (19)$$

where the weights ω_k 's, which generally depend on α and θ , are generated by the function $\omega(\zeta)$:

$$\omega(\zeta) = \left[\frac{1-\zeta}{\frac{1}{2}(1+\zeta) + \frac{\theta}{\alpha}(1-\zeta)} \right]^\alpha, \quad 0 < \theta \leq \frac{1}{2}. \quad (20)$$

We also introduce a new sequence $\{\varpi_k\}_{k=0}^\infty$ aiming to facilitate the following analysis, i.e., define

$$\varpi(\zeta) = \sum_{k=0}^\infty \varpi_k \zeta^k := \frac{1-\zeta}{\omega(\zeta)} = (1-\zeta)^{1-\alpha} \left[\frac{1}{2}(1+\zeta) + \frac{\theta}{\alpha}(1-\zeta) \right]^\alpha. \quad (21)$$

Lemma 3.1. *For $\alpha \in (0, 1)$ and $\theta \in (0, \frac{1}{2}]$, the sequence $\{\varpi_k\}_{k=0}^\infty$ fulfills the properties that (i) $\varpi_k = O(k^{\alpha-2})$ and (ii) $\tau^{-(1-\alpha)} e^{(\frac{1}{2}-\theta)\tau} \varpi(e^{-\tau}) = 1 + O(\tau^2)$.*

Proof. Let $\nu(\zeta) := \left[\frac{1}{2}(1+\zeta) + \frac{\theta}{\alpha}(1-\zeta) \right]^\alpha$ and thus $\varpi(\zeta) = (1-\zeta)^{1-\alpha} \nu(\zeta)$. The only singular point ζ_0 of $\nu(\zeta)$ is

$$\zeta_0 = 1 + \frac{1}{\frac{\theta}{\alpha} - \frac{1}{2}},$$

satisfying that $|\zeta_0| > 1$ due to the fact $\frac{\theta}{\alpha} > 0$. Then, $\nu(\zeta)$ is analytic on a closed unit disk in \mathbb{C} , indicating that the weights of the expansion of $\nu(\zeta)$ decay faster than $O(k^{-\ell})$ for any positive integer ℓ . The decay rate of the weights ϖ_k , as a discrete convolution of two sequences formed by the coefficients of expansion of $(1-\zeta)^{1-\alpha}$ and $\nu(\zeta)$ respectively, is totally determined by $(1-\zeta)^{1-\alpha}$, which confirms (i). To prove (ii), replace $e^{-\tau}$ and $e^{(\frac{1}{2}-\theta)\tau}$ with their Taylor expansions with respect to τ , followed by some simple calculations which are omitted here. \square

Remark 3.2. *The properties (i) and (ii) in the above lemma essentially imply the formula $\tau^{\alpha-1} \sum_{k=0}^n \varpi_k u^{n-k}$ can approximate $\partial_t^{1-\alpha} u$ at time $t_{n-\frac{1}{2}+\theta}$ with second-order accuracy. We refer to the shifted convolution quadrature in [37] for more information.*

Lemma 3.3. *For $\theta \in [\frac{\alpha}{2}, \frac{1}{2}]$, the weights ϖ_k satisfy (i) $\varpi_0 > 0$, (ii) $\varpi_k \leq 0$, $k \geq 1$.*

Proof. We present first a recursive formula for calculating ϖ_k . Let $\zeta = 0$ in (21) and thus $\varpi_0 = \varpi(0) = \left(\frac{1}{2} + \frac{\theta}{\alpha}\right)^\alpha > 0$ which confirms (i). Take the first derivative of $\varpi(\zeta)$ with respect to ζ and multiply both sides of the resultant by $(1-\zeta) \left[\frac{1}{2}(1+\zeta) + \frac{\theta}{\alpha}(1-\zeta) \right]$, to obtain

$$(1-\zeta) \left[\frac{1}{2}(1+\zeta) + \frac{\theta}{\alpha}(1-\zeta) \right] \varpi'(\zeta) = \left[\left(\frac{\theta}{\alpha} - \frac{1}{2} \right) \zeta + \alpha - \frac{\theta}{\alpha} - \frac{1}{2} \right] \varpi(\zeta). \quad (22)$$

Considering that $\varpi(\zeta) = \sum_{k=0}^\infty \varpi_k \zeta^k$ and $\varpi'(\zeta) = \sum_{k=1}^\infty k \varpi_k \zeta^{k-1}$, by comparing the coefficient of ζ^k of the expansion of both sides of (22), we have

$$\varpi_1 = \frac{\alpha - \frac{\theta}{\alpha} - \frac{1}{2}}{\frac{\theta}{\alpha} + \frac{1}{2}} \varpi_0 \leq \frac{\alpha - 1}{\frac{\theta}{\alpha} + \frac{1}{2}} \varpi_0 < 0, \quad \text{since } \theta \geq \frac{\alpha}{2}, \quad (23)$$

and for $k \geq 2$,

$$\varpi_k = \frac{1}{\left(\frac{\theta}{\alpha} + \frac{1}{2}\right)k} \left\{ \left[\frac{\theta}{\alpha}(2k-3) + \alpha - \frac{1}{2} \right] \varpi_{k-1} + \left(\frac{\theta}{\alpha} - \frac{1}{2} \right) (3-k) \varpi_{k-2} \right\}. \quad (24)$$

Next we prove that if $k \geq 4$, there holds

$$\frac{\varpi_{k-1}}{\varpi_{k-2}} \geq \rho_{k-1} > \frac{\left(\frac{\theta}{\alpha} - \frac{1}{2}\right)(k-3)}{\frac{\theta}{\alpha}(2k-3) + \alpha - \frac{1}{2}}, \quad (25)$$

where $\rho(\alpha, \theta, k) = \frac{\left(\frac{\theta}{\alpha} - \frac{1}{2}\right)(k-2)}{\frac{\theta}{\alpha}(2k-1) + \alpha - \frac{1}{2}} \frac{4\theta}{2\theta + \alpha} \left(1 + \frac{1}{k}\right)$. Note that the correctness of the second inequality of (25) is obvious. By letting $k = 3$ in (24), we have $\frac{\varpi_3}{\varpi_2} = \left(\frac{3\theta}{\alpha} + \alpha - \frac{1}{2}\right) / \left(\frac{3\theta}{\alpha} + \frac{3}{2}\right)$ and

$$\begin{aligned} \frac{\varpi_3}{\varpi_2} - \rho_3 &= \frac{4\alpha^4 - 4\alpha^3 + (32\theta + 1)\alpha^2 + 28\theta^2}{3(\alpha + 2\theta)(2\alpha^2 - \alpha + 10\theta)} \\ &\geq \frac{4\alpha^4 + 12\alpha^3 + 8\alpha^2}{3(\alpha + 2\theta)(2\alpha^2 - \alpha + 10\theta)} > 0. \end{aligned} \quad (26)$$

Now, assume (25) is true for $k = 4, 5, \dots, m (m \geq 4)$. For $k = m + 1$, we derive from (24) that

$$\frac{\varpi_m}{\varpi_{m-1}} = \frac{1}{\left(\frac{\theta}{\alpha} + \frac{1}{2}\right)m} \left[\frac{\theta}{\alpha}(2m-3) + \alpha - \frac{1}{2} + \left(\frac{\theta}{\alpha} - \frac{1}{2}\right)(3-m) \frac{\varpi_{m-2}}{\varpi_{m-1}} \right], \quad (27)$$

which, combined with the assumption, leads to

$$\begin{aligned} \frac{\varpi_m}{\varpi_{m-1}} &\geq \frac{1}{\left(\frac{\theta}{\alpha} + \frac{1}{2}\right)m} \left[\frac{\theta}{\alpha}(2m-3) + \alpha - \frac{1}{2} + \left(\frac{\theta}{\alpha} - \frac{1}{2}\right)(3-m) \frac{1}{\rho_{m-1}} \right] \\ &= \frac{1}{\left(\frac{\theta}{\alpha} + \frac{1}{2}\right)m} \left[\frac{\theta}{\alpha}(2m-3) + \alpha - \frac{1}{2} \right] \left(1 + \frac{2\theta + \alpha}{4\theta} \frac{m-1}{m} \right) \\ &=: \tilde{\rho}(\alpha, \theta, m). \end{aligned} \quad (28)$$

To avoid tedious calculation, we shall numerically show that $\tilde{\rho}(\alpha, \theta, m) \geq \rho(\alpha, \theta, m)$. Let $m = \frac{4}{x}$ for some $x \in (0, 1]$, and define a function $\Theta(x, \alpha, \theta)$ in $\Sigma = \{(x, \alpha, \theta) : x \in (0, 1], \alpha \in (0, 1), \theta \in [\frac{\alpha}{2}, \frac{1}{2}]\}$, such that $\Theta(x, \alpha, \theta) = \tilde{\rho}(\alpha, \theta, \frac{4}{x}) - \rho(\alpha, \theta, \frac{4}{x})$. Fig.1 illustrates the values $\min_{\theta \in [\frac{\alpha}{2}, \frac{1}{2}]} \Theta(x, \alpha, \theta)$ for $(x, \alpha) \in (0, 1] \times (0, 1)$, which indicates the positivity of $\min_{\theta \in [\frac{\alpha}{2}, \frac{1}{2}]} \Theta(x, \alpha, \theta)$ and further $\tilde{\rho}(\alpha, \theta, m) \geq \rho(\alpha, \theta, m)$. Therefore, combining (26)-(28) we justify (25) by induction.

Finally, by (24) and (25), we derive for $k \geq 4$,

$$\varpi_k = \frac{\varpi_{k-1}}{\left(\frac{\theta}{\alpha} + \frac{1}{2}\right)k} \left\{ \left[\frac{\theta}{\alpha}(2k-3) + \alpha - \frac{1}{2} \right] + \left(\frac{\theta}{\alpha} - \frac{1}{2}\right)(3-k) \frac{\varpi_{k-2}}{\varpi_{k-1}} \right\} < 0, \quad (29)$$

provided $\varpi_{k-1} < 0$. Direct calculations from (24) show that

$$\varpi_2 = \frac{\alpha(\alpha-1)}{2\left(\frac{\theta}{\alpha} + \frac{1}{2}\right)^2} \varpi_0 < 0, \quad \text{and} \quad \varpi_3 = \frac{1}{3\left(\frac{\theta}{\alpha} + \frac{1}{2}\right)} \left(\frac{3\theta}{\alpha} + \alpha - \frac{1}{2} \right) \varpi_2 < 0. \quad (30)$$

Then, the results (23), (29) and (30) validate (ii), which complete the proof of the lemma. \square

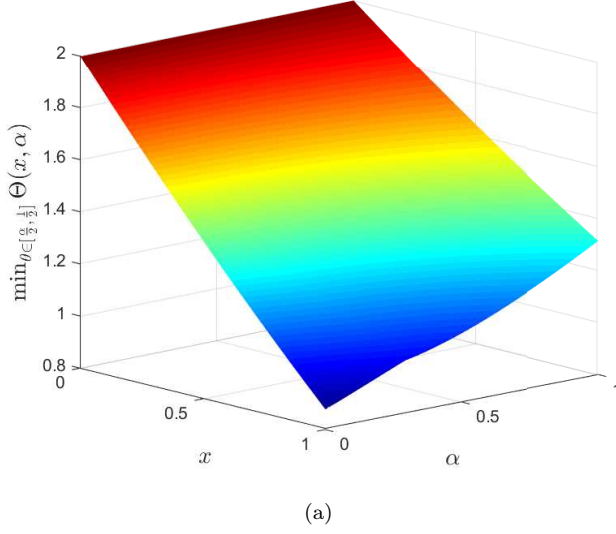


Figure 1: Values of $\min_{\theta \in [\frac{\alpha}{2}, \frac{1}{2}]} \Theta(x, \alpha, \theta)$ for $(x, \alpha) \in (0, 1] \times (0, 1)$.

Remark 3.4. We emphasize that the condition $\theta \in [\frac{\alpha}{2}, \frac{1}{2}]$ in the above lemma is not necessary to guarantee (i) and (ii), however, the negativity of ϖ_1 in (23) actually requires $\theta > \alpha(\alpha - \frac{1}{2})$, meaning that $\theta \geq \frac{1}{2}$ (and therefore $\theta = \frac{1}{2}$ due to (20)) when $\alpha \rightarrow 1$, which is still compatible to our condition $\theta \in [\frac{\alpha}{2}, \frac{1}{2}]$.

Lemma 3.5. Let $\theta \in [\frac{\alpha}{2}, \frac{1}{2}]$. Assume $v_0 = 0$. For any sequence $(v_1, v_2, \dots, v_n) \in \mathbb{R}^n, n \geq 1$, there holds

$$v^n \sum_{k=1}^n \varpi_{n-k} v^k \geq \frac{1}{2} \sum_{k=1}^n a_{n-k} [(v^k)^2 - (v^{k-1})^2] + \frac{1}{2\varpi_0} \left\| \sum_{k=1}^n \varpi_{n-k} v^k \right\|^2, \quad (31)$$

where $a_j = \sum_{k=0}^j \varpi_k$.

Proof. Denote by $\nabla_\tau v^k := v^k - v^{k-1}$ for $k \geq 1$. Then, $v^k = \sum_{j=1}^k \nabla_\tau v^j$ and

$$\sum_{k=1}^n \varpi_{n-k} v^k = \sum_{k=1}^n \varpi_{n-k} \sum_{j=1}^k \nabla_\tau v^j = \sum_{j=1}^n \nabla_\tau v^j \sum_{k=j}^n \varpi_{n-k} = \sum_{j=1}^n a_{n-j} \nabla_\tau v^j.$$

By Lemma 3.3 and the fact $\sum_{k=1}^\infty \varpi_k = 0$, one can directly get

$$a_0 \geq a_1 \geq a_2 \geq \dots \geq a_{n-1} > 0, \quad \text{for any } n \geq 1, \quad (32)$$

followed by the inequality (31) according to Lemma A.1 of [38]. \square

Remark 3.6. For the sequence $\{a_j\}_{j=0}^\infty$ defined in the above lemma, there holds

$$a(\zeta) = \sum_{j=0}^\infty a_j \zeta^j = \sum_{j=0}^\infty \left(\sum_{k=0}^j \varpi_k \right) \zeta^j = \frac{\varpi(\zeta)}{1-\zeta} = \frac{1}{\omega(\zeta)} = (1-\zeta)^{-\alpha} \left[\frac{1}{2}(1+\zeta) + \frac{\theta}{\alpha}(1-\zeta) \right]^\alpha.$$

By quite similar analysis as that of Lemma 3.1, we can get (i) $a_k = O(k^{\alpha-1})$ and (ii) $\tau^\alpha e^{-\theta\tau} a(e^{-\tau}) = 1 + O(\tau^2)$. If we define $\mathcal{I}_\tau^{\alpha,\theta} u^n := \tau^\alpha \sum_{k=0}^n a_k u^{n-k}$, then (i) and (ii) indicate that $\mathcal{I}_\tau^{\alpha,\theta} u^n$ approximates $\mathcal{I}^\alpha u$ at time $t = t_{n+\theta}$ with second-order accuracy (see [37, Theorem 1]).

The time semi-discrete θ -scheme for (1)-(3) then reads: For given \mathbf{E}^0, H^0 and \mathbf{P}^0 , find $\mathbf{E}_\tau^n \in H_0(\text{curl}; \Omega) \cap (L^2(\Omega))^2$, $H_\tau^n \in L^2(\Omega)$ and $\mathbf{P}_\tau^n \in (L^2(\Omega))^2$ with $n \geq 1$ such that

$$\epsilon_0 \epsilon_\infty (\partial_\tau^{n-\theta} \mathbf{E}_\tau, \boldsymbol{\chi}) + (\partial_\tau^{n-\theta} \mathbf{P}_\tau, \boldsymbol{\chi}) - (\overline{H}_\tau^{n-\theta}, \nabla \times \boldsymbol{\chi}) = 0, \quad \forall \boldsymbol{\chi} \in H_0(\text{curl}; \Omega), \quad (33)$$

$$\mu_0 (\partial_\tau^{n-\theta} H_\tau, \phi) + (\nabla \times \overline{\mathbf{E}}_\tau^{n-\theta}, \phi) = 0, \quad \forall \phi \in L^2(\Omega), \quad (34)$$

$$\tau_0^\alpha (\partial_\tau^\alpha \mathbf{P}_\tau^{n-\theta}, \boldsymbol{\psi}) + (\overline{\mathbf{P}}_\tau^{n-\theta}, \boldsymbol{\psi}) - \epsilon_0 (\epsilon_s - \epsilon_\infty) (\overline{\mathbf{E}}_\tau^{n-\theta}, \boldsymbol{\psi}) = 0, \quad \forall \boldsymbol{\psi} \in (L^2(\Omega))^2. \quad (35)$$

Theorem 3.7. For arbitrary $\theta \in [\frac{\alpha}{2}, \frac{1}{2}]$ with $\alpha \in (0, 1)$ and any $\tau > 0$, the semidiscrete scheme (33)-(35) fulfills the discrete energy dissipation:

$$\tilde{\mathcal{E}}_\alpha^n \leq \tilde{\mathcal{E}}_\alpha^{n-1}, \quad \text{for } n \geq 1, \quad (36)$$

where $\tilde{\mathcal{E}}_\alpha^n := \tau_0^\alpha \mathcal{I}_\tau^{\alpha,\theta} \|\partial_\tau^\alpha \mathbf{P}_\tau^{n-\theta}\|^2 + \|\mathbf{P}_\tau^n\|^2 + \epsilon_0 (\epsilon_s - \epsilon_\infty) (\epsilon_0 \epsilon_\infty \|\mathbf{E}_\tau^n\|^2 + \mu_0 \|H_\tau^n\|^2)$ is the discrete counterpart of the continuous energy $\mathcal{E}_\alpha(t_n)$.

Proof. Let $\boldsymbol{\chi} = \overline{\mathbf{E}}_\tau^{n-\theta}$ in (33) and $\phi = \overline{H}_\tau^{n-\theta}$ in (34), respectively, and add these two equation together to obtain

$$\frac{1}{2} \epsilon_0 \epsilon_\infty \partial_\tau^{n-\theta} \|\mathbf{E}_\tau\|^2 + \frac{\mu_0}{2} \partial_\tau^{n-\theta} \|H_\tau\|^2 + (\partial_\tau^{n-\theta} \mathbf{P}_\tau, \overline{\mathbf{E}}_\tau^{n-\theta}) \leq 0, \quad (37)$$

where we have used the fact that $(a-b)((1-\theta)a + \theta b) \geq \frac{1}{2}(a^2 - b^2)$ provided $\theta \in (0, \frac{1}{2}]$. Replace $\boldsymbol{\psi}$ in (35) by $\partial_\tau^{n-\theta} \mathbf{P}_\tau$ and add the result to (37) after multiplying (37) by $\epsilon_0 (\epsilon_s - \epsilon_\infty)$, to get

$$\tau_0^\alpha (\partial_\tau^\alpha \mathbf{P}_\tau^{n-\theta}, \partial_\tau^{n-\theta} \mathbf{P}_\tau) + \frac{1}{2} \partial_\tau^{n-\theta} \|\mathbf{P}_\tau\|^2 + \frac{1}{2} \epsilon_0 (\epsilon_s - \epsilon_\infty) (\epsilon_0 \epsilon_\infty \partial_\tau^{n-\theta} \|\mathbf{E}_\tau\|^2 + \mu_0 \partial_\tau^{n-\theta} \|H_\tau\|^2) \leq 0. \quad (38)$$

then, using the weights ϖ_k one can immediately obtain

$$\partial_\tau^{n-\theta} \mathbf{P}_\tau = \tau^{\alpha-1} \sum_{k=1}^n \varpi_{n-k} (\partial_\tau^\alpha \mathbf{P}_\tau^{k-\theta}). \quad (39)$$

By Lemma 3.5, the first term of (38) reads

$$\begin{aligned} (\partial_\tau^\alpha \mathbf{P}_\tau^{n-\theta}, \partial_\tau^{n-\theta} \mathbf{P}_\tau) &= \tau^{\alpha-1} \left(\partial_\tau^\alpha \mathbf{P}_\tau^{n-\theta}, \sum_{k=1}^n \varpi_{n-k} (\partial_\tau^\alpha \mathbf{P}_\tau^{k-\theta}) \right) \\ &\geq \frac{\tau^{\alpha-1}}{2} \sum_{k=1}^n a_{n-k} [\|\partial_\tau^\alpha \mathbf{P}_\tau^{k-\theta}\|^2 - \|\partial_\tau^\alpha \mathbf{P}_\tau^{k-1-\theta}\|^2] + \frac{\tau^{\alpha-1}}{2\varpi_0} \left\| \sum_{k=1}^n \varpi_{n-k} (\partial_\tau^\alpha \mathbf{P}_\tau^{k-\theta}) \right\|^2 \\ &= \frac{\tau^{\alpha-1}}{2} \sum_{k=1}^n a_{n-k} \|\partial_\tau^\alpha \mathbf{P}_\tau^{k-\theta}\|^2 - \frac{\tau^{\alpha-1}}{2} \sum_{k=1}^{n-1} a_{n-1-k} \|\partial_\tau^\alpha \mathbf{P}_\tau^{k-\theta}\|^2 + \frac{\tau^{\alpha-1}}{2\varpi_0} \left\| \sum_{k=1}^n \varpi_{n-k} (\partial_\tau^\alpha \mathbf{P}_\tau^{k-\theta}) \right\|^2 \\ &= \frac{1}{2\tau} (\mathcal{I}_\tau^{\alpha,\theta} \|\partial_\tau^\alpha \mathbf{P}_\tau^{n-\theta}\|^2 - \mathcal{I}_\tau^{\alpha,\theta} \|\partial_\tau^\alpha \mathbf{P}_\tau^{n-1-\theta}\|^2) + \frac{\tau^{\alpha-1}}{2\varpi_0} \left\| \sum_{k=1}^n \varpi_{n-k} (\partial_\tau^\alpha \mathbf{P}_\tau^{k-\theta}) \right\|^2. \end{aligned} \quad (40)$$

Finally, combining (38), (39) with (40), one can get

$$\partial_\tau^{n-\theta} \tilde{\mathcal{E}}_\alpha + \tau_0^\alpha \frac{\tau^{1-\alpha}}{\varpi_0} \|\partial_\tau^{n-\theta} \mathbf{P}_\tau\|^2 \leq 0, \quad (41)$$

meaning that $\partial_\tau^{n-\theta} \tilde{\mathcal{E}}_\alpha \leq 0$, which completes the proof of the theorem. \square

4. Error Analysis

In this section, we consider the convergence rate of the semi-discrete scheme by assuming the solution is smooth enough. Source terms are added to the Cole-Cole model, reading that

$$\epsilon_0 \epsilon_\infty \frac{\partial \mathbf{E}}{\partial t}(\mathbf{x}, t) = \nabla \times H(\mathbf{x}, t) - \frac{\partial \mathbf{P}}{\partial t}(\mathbf{x}, t) + \mathbf{f}_1(\mathbf{x}, t), \quad (42)$$

$$\mu_0 \frac{\partial H}{\partial t}(\mathbf{x}, t) = -\nabla \times \mathbf{E}(\mathbf{x}, t) + f_2(\mathbf{x}, t), \quad (43)$$

$$\tau_0^\alpha \partial_t^\alpha \mathbf{P}(\mathbf{x}, t) + \mathbf{P}(\mathbf{x}, t) = \epsilon_0(\epsilon_s - \epsilon_\infty) \mathbf{E}(\mathbf{x}, t) + \mathbf{f}_3(\mathbf{x}, t). \quad (44)$$

The time semi-discrete scheme is formulated as

$$\epsilon_0 \epsilon_\infty \partial_\tau^{n-\theta} \mathbf{E}_\tau + \partial_\tau^{n-\theta} \mathbf{P}_\tau - \nabla \times \overline{\mathbf{H}}_\tau^{n-\theta} = \mathbf{f}_1(\mathbf{x}, t_{n-\theta}), \quad (45)$$

$$\mu_0 \partial_\tau^{n-\theta} H_\tau + \nabla \times \overline{\mathbf{E}}_\tau^{n-\theta} = f_2(\mathbf{x}, t_{n-\theta}), \quad (46)$$

$$\tau_0^\alpha \partial_\tau^\alpha \mathbf{P}_\tau^{n-\theta} + \overline{\mathbf{P}}_\tau^{n-\theta} - \epsilon_0(\epsilon_s - \epsilon_\infty) \overline{\mathbf{E}}_\tau^{n-\theta} = \mathbf{f}_3(\mathbf{x}, t_{n-\theta}). \quad (47)$$

The following theorem demonstrates that the temporal accuracy of the energy-dissipation-preserving scheme is of order $O(\tau)$ when $\theta \neq \frac{1}{2}$, and improves to $O(\tau^2)$ when $\theta = \frac{1}{2}$.

Theorem 4.1. *Let $(\mathbf{E}(t), \mathbf{P}(t), H(t))$ be the solution of (1)-(3) where $\mathbf{E} \in C(0, T; H_0(\text{curl}; \Omega)) \cap C^3(0, T; (L^2(\Omega))^2)$, $\mathbf{P} \in C^3(0, T; (L^2(\Omega))^2)$ and $H \in C^3(0, T; H_0(\text{curl}; \Omega))$. Let $(\mathbf{E}_\tau^n, \mathbf{P}_\tau^n, H_\tau^n)$ be the solution of the time semi-discrete scheme (33)-(35). For sufficiently small τ there holds that*

$$\max_{n \geq 1} (\|\mathbf{E}^n - \mathbf{E}_\tau^n\| + \|\mathbf{P}^n - \mathbf{P}_\tau^n\| + \|H^n - H_\tau^n\|) \leq C\tau^s, \quad s = \begin{cases} 1, & \text{if } \theta \in [\frac{\alpha}{2}, \frac{1}{2}), \\ 2, & \text{if } \theta = \frac{1}{2}, \end{cases} \quad (48)$$

where C is a constant independent of τ .

Proof. Rewrite the Cole-Cole model with source terms (42)-(44) into the following form

$$\epsilon_0 \epsilon_\infty \partial_\tau^{n-\theta} \mathbf{E} + \partial_\tau^{n-\theta} \mathbf{P} - \nabla \times \overline{\mathbf{H}}^{n-\theta} = \mathbf{f}_1(\mathbf{x}, t_{n-\theta}) + \mathbf{R}_1^{n-\theta}, \quad (49)$$

$$\mu_0 \partial_\tau^{n-\theta} H + \nabla \times \overline{\mathbf{E}}^{n-\theta} = f_2(\mathbf{x}, t_{n-\theta}) + R_2^{n-\theta}, \quad (50)$$

$$\tau_0^\alpha \partial_\tau^\alpha \mathbf{P}^{n-\theta} + \overline{\mathbf{P}}^{n-\theta} - \epsilon_0(\epsilon_s - \epsilon_\infty) \overline{\mathbf{E}}^{n-\theta} = \mathbf{f}_3(\mathbf{x}, t_{n-\theta}) + \mathbf{R}_3^{n-\theta}, \quad (51)$$

where the error terms are defined by

$$\begin{aligned}
\mathbf{R}_1^{n-\theta} &= \epsilon_0 \epsilon_\infty \left(\partial_\tau^{n-\theta} \mathbf{E} - \frac{\partial \mathbf{E}}{\partial t}(\mathbf{x}, t_{n-\theta}) \right) + \left(\partial_\tau^{n-\theta} \mathbf{P} - \frac{\partial \mathbf{P}}{\partial t}(\mathbf{x}, t_{n-\theta}) \right) \\
&\quad - \nabla \times (\overline{H}^{n-\theta} - H(\mathbf{x}, t_{n-\theta})), \\
\mathbf{R}_2^{n-\theta} &= \mu_0 \left(\partial_\tau^{n-\theta} H - \frac{\partial H}{\partial t}(\mathbf{x}, t_{n-\theta}) \right) + \nabla \times (\overline{\mathbf{E}}^{n-\theta} - \mathbf{E}(\mathbf{x}, t_{n-\theta})), \\
\mathbf{R}_3^{n-\theta} &= \tau_0^\alpha (\partial_\tau^\alpha \mathbf{P}^{n-\theta} - \partial_t^\alpha \mathbf{P}(\mathbf{x}, t_{n-\theta})) - \epsilon_0 (\epsilon_s - \epsilon_\infty) (\overline{\mathbf{E}}^{n-\theta} - \mathbf{E}(\mathbf{x}, t_{n-\theta})).
\end{aligned} \tag{52}$$

It is clear that $\|\mathbf{R}_1^{n-\theta}\| + \|\mathbf{R}_2^{n-\theta}\| + \|\mathbf{R}_3^{n-\theta}\| = O(\tau^s)$ where $s = 1$ if $\theta \neq \frac{1}{2}$ and $s = 2$ if $\theta = \frac{1}{2}$. Let $\boldsymbol{\xi}_E^n := \mathbf{E}^n - \mathbf{E}_\tau^n$, $\xi_H^n := H^n - H_\tau^n$ and $\boldsymbol{\xi}_P^n := \mathbf{P}^n - \mathbf{P}_\tau^n$. Subtracting (45)-(47) from (49)-(51), one gets

$$\epsilon_0 \epsilon_\infty \partial_\tau^{n-\theta} \boldsymbol{\xi}_E + \partial_\tau^{n-\theta} \boldsymbol{\xi}_P - \nabla \times \overline{\xi}_H^{n-\theta} = \mathbf{R}_1^{n-\theta}, \tag{53}$$

$$\mu_0 \partial_\tau^{n-\theta} \xi_H + \nabla \times \overline{\boldsymbol{\xi}}_E^{n-\theta} = \mathbf{R}_2^{n-\theta}, \tag{54}$$

$$\tau_0^\alpha \partial_\tau^\alpha \boldsymbol{\xi}_P^{n-\theta} + \overline{\boldsymbol{\xi}}_P^{n-\theta} - \epsilon_0 (\epsilon_s - \epsilon_\infty) \overline{\boldsymbol{\xi}}_E^{n-\theta} = \mathbf{R}_3^{n-\theta}. \tag{55}$$

By similar arguments as the stability analysis in Theorem 3.7, we have

$$\begin{aligned}
&\tau^{1-\alpha} \|\partial_\tau^{n-\theta} \boldsymbol{\xi}_P\|^2 + \partial_\tau^{n-\theta} \|\boldsymbol{\xi}_P\|^2 + \partial_\tau^{n-\theta} \|\boldsymbol{\xi}_E\|^2 + \partial_\tau^{n-\theta} \|\xi_H\|^2 \\
&\leq C(\mathbf{R}_1^{n-\theta}, \overline{\boldsymbol{\xi}}_E^{n-\theta}) + C(R_2^{n-\theta}, \overline{\xi}_H^{n-\theta}) + C(\mathbf{R}_3^{n-\theta}, \partial_\tau^{n-\theta} \boldsymbol{\xi}_P).
\end{aligned} \tag{56}$$

Multiply both hand-side of (56) by τ , replace n with j and sum the index j from 1 to n to obtain

$$\begin{aligned}
&\|\boldsymbol{\xi}_P^n\|^2 + \|\boldsymbol{\xi}_E^n\|^2 + \|\xi_H^n\|^2 \\
&\leq C\tau \sum_{j=1}^n \left((\mathbf{R}_1^{j-\theta}, \overline{\boldsymbol{\xi}}_E^{j-\theta}) + (R_2^{j-\theta}, \overline{\xi}_H^{j-\theta}) + (\mathbf{R}_3^{j-\theta}, \partial_\tau^{j-\theta} \boldsymbol{\xi}_P) \right).
\end{aligned} \tag{57}$$

Based on the identity

$$(\mathbf{R}_3^{j-\theta}, \partial_\tau^{j-\theta} \boldsymbol{\xi}_P) = \frac{1}{\tau} [(\mathbf{R}_3^{j-\theta}, \boldsymbol{\xi}_P^j) - (\mathbf{R}_3^{j-1-\theta}, \boldsymbol{\xi}_P^{j-1})] - (\partial_{\tau,\theta}^j \mathbf{R}_3, \boldsymbol{\xi}_P^{j-1}) \tag{58}$$

where $\partial_{\tau,\theta}^j \mathbf{R}_3 := \frac{1}{\tau} (\mathbf{R}_3^{j-\theta} - \mathbf{R}_3^{j-\theta-1})$. For sufficiently smooth \mathbf{P} and \mathbf{E} , it holds that $\|\partial_{\tau,\theta}^j \mathbf{R}_3\| = O(\tau^s)$. Applying the Cauchy-Schwarz and Young inequalities, (57) and (58) yield

$$\|\boldsymbol{\xi}_P^n\|^2 + \|\boldsymbol{\xi}_E^n\|^2 + \|\xi_H^n\|^2 \leq C\tau \sum_{j=1}^n (\|\boldsymbol{\xi}_P^j\|^2 + \|\boldsymbol{\xi}_E^j\|^2 + \|\xi_H^j\|^2) + O(\tau^{2s}). \tag{59}$$

Finally, using the Gronwall inequality, we complete the proof of the theorem. \square

Remark 4.2. *The fully discrete scheme can be directly formulated using the Nédélec element, and its error analysis follows straightforwardly. For completeness, we refer the reader to [30] for details, as these aspects fall outside the scope of this paper.*

5. Numerical tests

In this section, we perform numerical tests to validate the theoretical findings regarding the energy-decay property and convergence rates.

5.1. C-C model with source terms

We consider the domain $\Omega = (0, 1)^2$ and final time $T = 1$, with the parameter values specified by $\epsilon_0 \epsilon_\infty = \mu_0 = \tau_0 = \epsilon_0(\epsilon_s - \epsilon_\infty) = 1$. For the purpose of convergence verification, the following smooth functions are prescribed as the exact solutions:

$$\begin{aligned} \mathbf{E}(x, y, t) &= e^{-t} \begin{pmatrix} (x^2 + 1) \sin(\pi y) \\ \sin(\pi x)(y - \frac{1}{2}) \end{pmatrix}, & \mathbf{P}(x, y, t) &= t^3 \begin{pmatrix} (x^2 + 1)y(y - 1) \\ x(x - 1)(y - \frac{1}{2}) \end{pmatrix}, \\ H(x, y, t) &= e^{-t}(x^3 + 1)(y^3 + 1). \end{aligned} \quad (60)$$

The corresponding source terms are subsequently derived from these defined solutions.

As a comparative benchmark, we approximate the term $\partial_t^\alpha \mathbf{P}(\mathbf{x}, t_{n-\theta})$ using alternative approaches as follows:

$$\begin{aligned} \partial_t^\alpha \mathbf{P}(\mathbf{x}, t_{n-\theta}) &= (1 - \theta) \partial_t^\alpha \mathbf{P}(\mathbf{x}, t_n) + \theta \partial_t^\alpha \mathbf{P}(\mathbf{x}, t_{n-1}) + O(\tau^2) \\ &= \tau^{-\alpha} \sum_{k=0}^n [(1 - \theta) \tilde{\omega}_{n-k} + \theta \tilde{\omega}_{n-k-1}] \mathbf{P}(\mathbf{x}, t_k) + O(\tau^2), \end{aligned} \quad (61)$$

where the coefficients $\tilde{\omega}_k$ are generated from the fractional BDF-2 scheme [39] via the generating function $\tilde{\omega}(\zeta) = (\frac{3}{2} - 2\zeta + \frac{1}{2}\zeta^2)^\alpha$.

For notational clarity, we refer to the numerical scheme proposed in this paper as **SFTR- θ** , and denote the alternative scheme based on approximation (61) as **F-BDF-2**. Define the error at time step n for \mathbf{E} as $\text{Error}_{\mathbf{E}^n} := \|\mathbf{E}^n - \mathbf{E}_\tau^n\|$. The corresponding global error in time is then given by $\text{Error}_{\mathbf{E}} := \max_n \text{Error}_{\mathbf{E}^n}$. The quantities \mathbf{P} and H are treated analogously.

The numerical results presented in Tables 1 and 2 validate the temporal convergence properties of two numerical schemes for solving the C-C model: the SFTR- θ method (Table 1) and the F-BDF-2 method (Table 2). Both tables display the global errors and corresponding convergence rates for the electric field (\mathbf{E}), magnetic field (H), and polarization (\mathbf{P}) with a fixed spatial discretization $h = \sqrt{2}/100$ and varying time steps τ . The data confirm the theoretical convergence orders for both schemes. When $\theta \neq 0.5$, first-order convergence is generally observed, particularly for smaller values of α . When $\theta = 0.5$, both methods achieve second-order convergence as expected. For $\theta \neq 0.5$, both schemes occasionally exhibit convergence rates exceeding the theoretical first-order prediction, particularly at larger α values.

5.2. C-C model without source terms

In this example, let $\Omega = (0, 1)^2$, $T = 1$, and set parameter values $\epsilon_0 \epsilon_\infty = \mu_0 = \tau_0 = \epsilon_0(\epsilon_s - \epsilon_\infty) = 1$. Choose the following initial conditions for the initial C-C model (1)-(3):

$$\mathbf{E}_0(x, y) = \begin{pmatrix} (x^2 + 1) \sin(\pi y) \\ \sin(\pi x)(y - \frac{1}{2}) \end{pmatrix}, \quad \mathbf{P}_0(x, y) = \mathbf{0}, \quad H_0(x, y) = (x^3 + 1)(y^3 + 1). \quad (62)$$

Figs. 2 and 3 present numerical experiments investigating the energy-decay properties of the SFTR- θ scheme and F-BDF-2 method. Fig. 2 demonstrates that the SFTR- θ scheme maintains strict monotonic energy-decay across various parameter values. Subfigure (a) shows consistent decay for $\alpha = 0.5$ with $\theta = 0.3, 0.4, 0.5$, while subfigure (b) confirms this property for $\theta = 0.5$

Table 1: Error and convergence rates for the SFTR- θ scheme with $h = \frac{\sqrt{2}}{100}$.

α	θ	τ	Error $_{\mathbf{E}}$	Rates	Error $_{\mathbf{H}}$	Rates	Error $_{\mathbf{P}}$	Rates
0.1	0.05	1/5	1.3051E-02		8.6135E-02		6.4191E-03	
		1/10	7.5273E-03	0.79	4.3739E-02	0.98	3.5507E-03	0.85
		1/20	4.0212E-03	0.90	2.2044E-02	0.99	1.8611E-03	0.93
		1/40	2.0713E-03	0.96	1.1069E-02	0.99	9.5010E-04	0.97
	0.5	1/5	7.7334E-03		1.2382E-02		1.2371E-02	
		1/10	2.4230E-03	1.67	4.1740E-03	1.57	4.7133E-03	1.39
		1/20	6.9085E-04	1.81	1.2611E-03	1.73	1.5101E-03	1.64
		1/40	1.8269E-04	1.92	3.4631E-04	1.86	4.2948E-04	1.81
0.5	0.25	1/5	9.0433E-03		4.6480E-02		4.6527E-03	
		1/10	4.9175E-03	0.88	2.3967E-02	0.96	1.9206E-03	1.28
		1/20	2.5560E-03	0.94	1.2169E-02	0.98	8.7310E-04	1.14
		1/40	1.3006E-03	0.97	6.1315E-03	0.99	4.1816E-04	1.06
	0.5	1/5	2.9735E-03		6.0447E-03		1.0138E-03	
		1/10	7.6690E-04	1.96	1.5668E-03	1.95	3.5522E-04	1.51
		1/20	1.9182E-04	2.00	3.9566E-04	1.99	1.0197E-04	1.80
		1/40	4.8005E-05	2.00	9.9517E-05	1.99	2.7168E-05	1.91
0.9	0.45	1/5	2.9562E-03		7.1173E-03		3.8101E-03	
		1/10	1.3316E-03	1.15	4.2064E-03	0.76	9.7433E-04	1.97
		1/20	6.3306E-04	1.07	2.2842E-03	0.88	2.6404E-04	1.88
		1/40	3.0873E-04	1.04	1.1893E-03	0.94	8.5076E-05	1.63
	0.5	1/5	1.6617E-03		4.1652E-03		3.1349E-03	
		1/10	4.1228E-04	2.01	1.0460E-03	1.99	7.7408E-04	2.02
		1/20	1.0253E-04	2.01	2.6175E-04	2.00	1.9240E-04	2.01
		1/40	2.5715E-05	2.00	6.5960E-05	1.99	4.7989E-05	2.00

Table 2: Error and convergence rates for the F-BDF-2 method with $h = \frac{\sqrt{2}}{100}$.

α	θ	τ	Error $_{\mathbf{E}}$	Rates	Error $_{\mathbf{H}}$	Rates	Error $_{\mathbf{P}}$	Rates
0.1	0.05	1/5	1.2990E-02		8.6118E-02		6.6458E-03	
		1/10	7.5131E-03	0.79	4.3736E-02	0.98	3.6152E-03	0.88
		1/20	4.0179E-03	0.90	2.2044E-02	0.99	1.8779E-03	0.94
		1/40	2.0705E-03	0.96	1.1069E-02	0.99	9.5437E-04	0.98
	0.5	1/5	2.0542E-03		4.7827E-03		1.6645E-03	
		1/10	5.0657E-04	2.02	1.1957E-03	2.00	4.3319E-04	1.94
		1/20	1.2693E-04	2.00	2.9866E-04	2.00	1.1051E-04	1.97
		1/40	3.1827E-05	2.00	7.5069E-05	1.99	2.7951E-05	1.98
0.5	0.25	1/5	8.5979E-03		4.6331E-02		6.7442E-03	
		1/10	4.8414E-03	0.83	2.3936E-02	0.95	2.4456E-03	1.46
		1/20	2.5424E-03	0.93	1.2162E-02	0.98	9.9213E-04	1.30
		1/40	1.2980E-03	0.97	6.1302E-03	0.99	4.4466E-04	1.16
	0.5	1/5	8.7112E-04		3.4754E-03		5.2863E-03	
		1/10	1.8965E-04	2.20	8.5412E-04	2.02	1.4162E-03	1.90
		1/20	5.1086E-05	1.89	2.1277E-04	2.01	3.6668E-04	1.95
		1/40	1.3673E-05	1.90	5.3786E-05	1.98	9.3296E-05	1.97
0.9	0.45	1/5	2.1597E-03		6.6744E-03		9.7369E-03	
		1/10	1.2583E-03	0.78	4.1196E-03	0.70	2.5996E-03	1.91
		1/20	6.3639E-04	0.98	2.2642E-03	0.86	6.7628E-04	1.94
		1/40	3.1195E-04	1.03	1.1846E-03	0.93	1.7900E-04	1.92
	0.5	1/5	9.4455E-04		3.7415E-03		9.7657E-03	
		1/10	3.1100E-04	1.60	9.7887E-04	1.93	2.6054E-03	1.91
		1/20	8.7175E-05	1.83	2.4558E-04	1.99	6.7213E-04	1.95
		1/40	2.3919E-05	1.87	6.1911E-05	1.99	1.7068E-04	1.98

with α ranging from 0.1 to 0.9. A smaller value of α leads to faster energy-decay in the vicinity of the initial time. Fig. 3 provides comparative analysis for $\theta = 0.5$ at different α values (0.2, 0.5, 0.8, 0.99). The SFTR- θ scheme preserves the discrete energy dissipation property $\tilde{\mathcal{E}}_\alpha^n \leq \tilde{\mathcal{E}}_\alpha^{n-1}$ in all cases. In contrast, the F-BDF-2 method exhibits non-physical energy oscillations and fails to maintain monotonic decay.

This distinction highlights the SFTR- θ scheme's superior capability in preserving the dissipative structure of the continuous model, ensuring numerical stability and physical fidelity in long-term simulations.

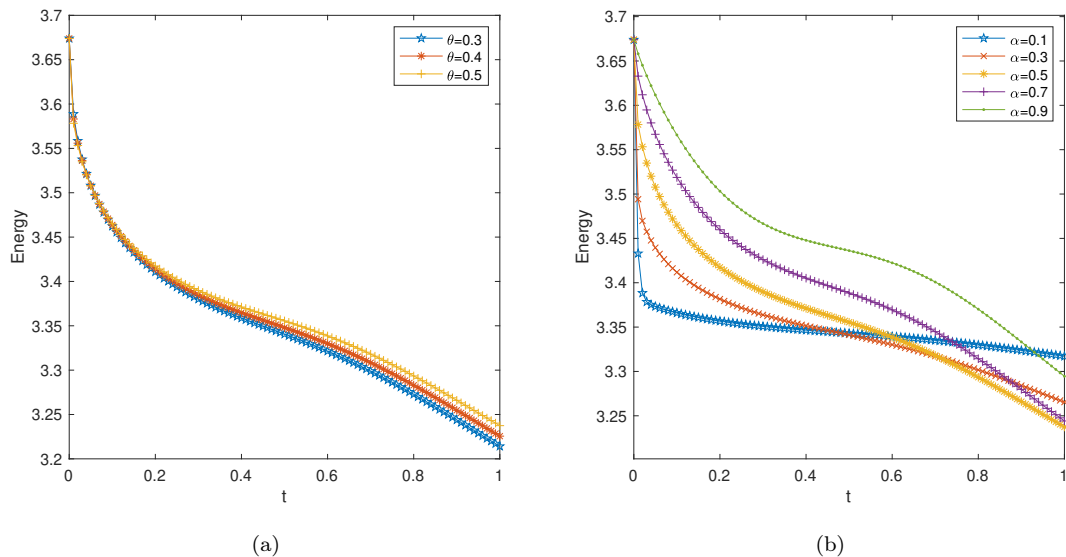


Figure 2: Illustration of the discrete energy-decay property of the SFTR- θ scheme with $h = \sqrt{2}/60$ and $\tau = 0.01$. (a) Energy evolution for $\alpha = 0.5$ with varying $\theta = 0.3, 0.4, 0.5$; (b) Energy evolution for $\theta = 0.5$ with varying $\alpha = 0.1, 0.3, 0.5, 0.7, 0.9$.

6. Conclusion

In this work, we have systematically studied the energy dissipation properties of the Cole–Cole model and developed a class of temporal discretization schemes that preserve discrete energy-decay. The main contributions are summarized as follows:

- A modified energy functional was introduced, and a rigorous proof of the energy-decay law for the continuous C-C model was established.
- A θ -scheme (SFTR- θ) was designed and analyzed, with a theoretical proof that it preserves the discrete energy-decay property under appropriate parameter choices.
- A detailed error analysis confirmed that the scheme achieves first-order convergence for $\theta \neq 0.5$ and second-order convergence for $\theta = 0.5$.
- Numerical tests verified the theoretical convergence rates and demonstrated the unconditional energy-decay behavior of the SFTR- θ scheme. In contrast, the F-BDF-2 method failed to preserve monotonic energy-decay in various settings.

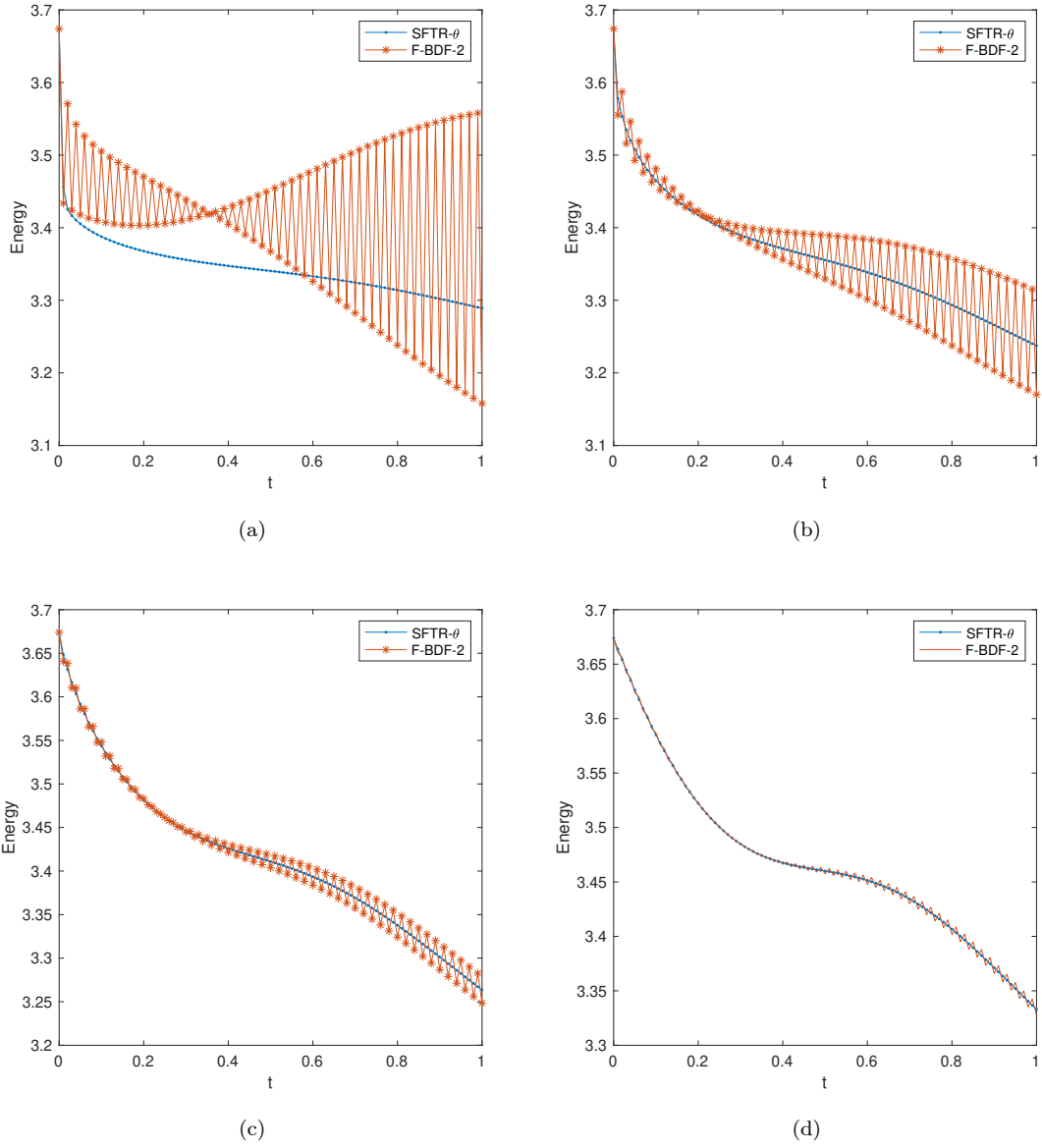


Figure 3: Comparison of the discrete energy-decay between the SFTR- θ scheme and the F-BDF-2 method, with parameters $h = \sqrt{2}/60$, $\tau = 0.01$, and $\theta = 0.5$: (a) $\alpha = 0.2$; (b) $\alpha = 0.5$; (c) $\alpha = 0.8$; (d) $\alpha = 0.99$.

The proposed scheme not only aligns with the physical dissipation structure of the C-C model but also provides a reliable foundation for adaptive time-stepping strategies in long-time simulations. Future work may extend this approach to more complex dispersive models such as the Havriliak-Negami model.

Declaration of competing interest

The authors declare no competing interests.

Acknowledgements

This work is supported by the National Natural Science Foundation of China (No. 12201322 to B.Y., No. 12401530 to G.Y., No. 12461080 to Y.L and No. 12561068 to H.L.), Scientific Research Project of Higher Education Institutions of Inner Mongolia Autonomous Region (No. NJZY23003 to Z. D.), Natural Science Foundation of Inner Mongolia (No. 2025MS01003 to B.Y.), Program for Innovative Research Team in Universities of Inner Mongolia Autonomous Region (No. NMGIRT2413 to Y.L.), Key Project of Natural Science Foundation of Inner Mongolia Autonomous Region (No. 2025ZD036 to H.L.).

References

- [1] K. Biswas, G. Bohannan, R. Caponetto, A. Mendes Lopes, J. A. Tenreiro Machado, Fractional-order models of vegetable tissues, in: *Fractional-Order Devices*, Springer, 2017, pp. 73–92.
- [2] J. Li, Y. Huang, Y. Lin, Developing finite element methods for Maxwell’s equations in a Cole–Cole dispersive medium, *SIAM J. Sci. Comput.* 33 (6) (2011) 3153–3174.
- [3] T. Repo, S. Pulli, Application of impedance spectroscopy for selecting frost hardy varieties of English ryegrass, *Ann. Bot.* 78 (5) (1996) 605–609.
- [4] C. Polk, E. Postow, *Handbook of Biological Effects of Electromagnetic Fields*, -2 Volume Set, CRC press, 1995.
- [5] C. Ionescu, A. Lopes, D. Copot, J. T. Machado, J. H. Bates, The role of fractional calculus in modeling biological phenomena: A review, *Commun. Nonlinear Sci. Numer. Simul.* 51 (2017) 141–159.
- [6] L. Liu, S. Chen, J. Yang, S. Zhang, L. Feng, X. Si, L. Zheng, Insight into the significance of absorbing boundary condition for the flow mechanism analysis of fractional Maxwell fluid over a semi-infinite plate, *Phys. Fluids* 35 (5).
- [7] R. W. Ziolkowski, E. Heyman, Wave propagation in media having negative permittivity and permeability, *Phys. Rev. E* 64 (5) (2001) 056625.
- [8] D. R. Smith, N. Kroll, Negative refractive index in left-handed materials, *Phys. Rev. Lett.* 85 (14) (2000) 2933.
- [9] S. Havriliak, S. Negami, A complex plane analysis of α -dispersions in some polymer systems, in: *Journal of Polymer Science Part C: Polymer Symposia*, Vol. 14, Wiley Online Library, 1966, pp. 99–117.

- [10] S. Havriliak, S. Negami, A complex plane representation of dielectric and mechanical relaxation processes in some polymers, *Polymer* 8 (1967) 161–210.
- [11] K. S. Cole, R. H. Cole, Dispersion and absorption in dielectrics I. Alternating current characteristics, *J. Chem. Phys.* 9 (4) (1941) 341–351.
- [12] S. Mustafa, A. M. Abbosh, P. T. Nguyen, Modeling human head tissues using fourth-order Debye model in convolution-based three-dimensional finite-difference time-domain, *IEEE Trans. Antennas Propag.* 62 (3) (2014) 1354–1361.
- [13] F. Torres, P. Vaudon, B. Jecko, Application of fractional derivatives to the FDTD modeling of pulse propagation in a Cole–Cole dispersive medium, *Microw. Opt. Technol. Lett.* 13 (5) (1996) 300–304.
- [14] A. Taflov, S. C. Hagness, M. Piket-May, Computational electromagnetics: the finite-difference time-domain method, *The Electrical Engineering Handbook* 3 (629–670) (2005) 15.
- [15] J. Schuster, R. Luebbers, An FDTD algorithm for transient propagation in biological tissue with a Cole-Cole dispersion relation, in: *IEEE Antennas and Propagation Society International Symposium. 1998 Digest. Antennas: Gateways to the Global Network. Held in conjunction with: USNC/URSI National Radio Science Meeting (Cat. No. 98CH36, Vol. 4, IEEE, 1998, pp. 1988–1991.*
- [16] M. F. Causley, P. G. Petropoulos, S. Jiang, Incorporating the Havriliak–Negami dielectric model in the FD-TD method, *J. Comput. Phys.* 230 (10) (2011) 3884–3899.
- [17] I. T. Rekanos, T. G. Papadopoulos, An auxiliary differential equation method for FDTD modeling of wave propagation in Cole-Cole dispersive media, *IEEE Trans. Antennas Propag.* 58 (11) (2010) 3666–3674.
- [18] J. Li, Y. Chen, Analysis of a time-domain finite element method for 3-D Maxwell’s equations in dispersive media, *Comput. Methods Appl. Mech. Eng.* 195 (33–36) (2006) 4220–4229.
- [19] D. Jiao, J.-M. Jin, Time-domain finite element modeling of dispersive media, in: *IEEE Antennas and Propagation Society International Symposium. 2001 Digest. Held in conjunction with: USNC/URSI National Radio Science Meeting (Cat. No. 01CH37229), Vol. 3, IEEE, 2001, pp. 180–183.*
- [20] H. T. Banks, V. Bokil, N. L. Gibson, Analysis of stability and dispersion in a finite element method for Debye and Lorentz dispersive media, *Numer. Methods Partial Differ. Equ.* 25 (4) (2009) 885–917.
- [21] Y. Yang, L.-L. Wang, F. Zeng, Analysis of a backward Euler-type scheme for Maxwell’s equations in a Havriliak–Negami dispersive medium, *ESAIM: Math. Model. Numer. Anal.* 55 (2) (2021) 479–506.
- [22] C. Huang, L.-L. Wang, An accurate spectral method for the transverse magnetic mode of Maxwell equations in Cole-Cole dispersive media, *Adv. Comput. Math.* 45 (2) (2019) 707–734.
- [23] J. Wang, J. Zhang, Z. Zhang, A CG-DG method for Maxwell’s equations in Cole-Cole dispersive media, *J. Comput. Appl. Math.* 393 (2021) 113480.

- [24] T. Lu, P. Zhang, W. Cai, Discontinuous Galerkin methods for dispersive and lossy Maxwell's equations and PML boundary conditions, *J. Comput. Phys.* 200 (2) (2004) 549–580.
- [25] L. Mescia, P. Bia, D. Caratelli, Fractional derivative based FDTD modeling of transient wave propagation in Havriliak–Negami media, *IEEE Trans. Microw. Theory Tech.* 62 (9) (2014) 1920–1929.
- [26] J. Chakarothai, Novel FDTD scheme for analysis of frequency-dependent medium using fast inverse Laplace transform and Prony's method, *IEEE Trans. Antennas Propag.* 67 (9) (2018) 6076–6089.
- [27] I. T. Rekanos, FDTD modeling of Havriliak–Negami media, *IEEE Microw. Wirel. Compon. Lett.* 22 (2) (2012) 49–51.
- [28] I. T. Rekanos, FDTD schemes for wave propagation in Davidson–Cole dispersive media using auxiliary differential equations, *IEEE Trans. Antennas Propag.* 60 (3) (2011) 1467–1478.
- [29] C. S. Antonopoulos, N. V. Kantartzis, I. T. Rekanos, FDTD method for wave propagation in Havriliak–Negami media based on fractional derivative approximation, *IEEE Trans. Magn.* 53 (6) (2017) 1–4.
- [30] B. Yin, Y. Liu, H. Li, Z. Zhang, On discrete energy dissipation of Maxwell's equations in a Cole–Cole dispersive medium, *J. Comput. Math.* 41 (5) (2023) 980–1002.
- [31] J. Xiao, D. Kong, An unconditionally stable second-order scheme for maxwell's equations in the cole–cole dispersive medium, *Applied Numerical Mathematics* 211 (2025) 211–227.
- [32] K. Diethelm, *The analysis of fractional differential equations: An application-oriented exposition using differential operators of Caputo type*, Springer Science & Business Media, 2010.
- [33] A. Alsaedi, B. Ahmad, M. Kirane, I. Mostefaoui, Maximum principle for certain generalized time and space fractional diffusion equations, *Quart. Appl. Math* 73 (1) (2015) 163–175.
- [34] H.-l. Liao, T. Tang, T. Zhou, An Energy Stable and Maximum Bound Preserving Scheme with Variable Time Steps for Time Fractional Allen–Cahn Equation, *SIAM J. Sci. Comput.* 43 (5) (2021) A3503–A3526.
- [35] B. Yin, Y. Liu, H. Li, Necessity of introducing non-integer shifted parameters by constructing high accuracy finite difference algorithms for a two-sided space-fractional advection–diffusion model, *Appl. Math. Lett.* 105 (2020) 106347.
- [36] B. Yin, Y. Liu, H. Li, Z. Zhang, Efficient shifted fractional trapezoidal rule for subdiffusion problems with nonsmooth solutions on uniform meshes, *BIT Numer. Math.* (2021) 1–36.
- [37] Y. Liu, B. Yin, H. Li, Z. Zhang, The unified theory of shifted convolution quadrature for fractional calculus, *J. Sci. Comput.* 89 (1) (2021) 1–24.
- [38] H.-l. Liao, W. McLean, J. Zhang, A discrete gronwall inequality with applications to numerical schemes for subdiffusion problems, *SIAM J. Numer. Anal.* 57 (1) (2019) 218–237.
- [39] C. Lubich, Discretized fractional calculus, *SIAM J. Math. Anal.* 17 (3) (1986) 704–719.